LEP Constraints on Neutralino Relic Densities, and the Fate of Higgsino Dark Matter

Toby Falk

Department of Physics, University of Wisconsin, Madison, WI 53706, USA

Abstract. We examine the current state of neutralino dark matter and consider how the LEP constraints on the Minimal Supersymmetric Standard Model parameters are squeezing the available dark matter regions. We also show how cosmological constraints augment bounds coming from collider searches to further constrain the MSSM parameter space.

1. Introduction

If R-parity is conserved, the Lightest Supersymmetric Particle (LSP) is stable. In many supersymmetric models, the LSP tends to have a cosmologically interesting relic density and is a good dark matter candidate [1, 2], and it is a very appealing feature of the Minimal Supersymmetric Standard Model that it can naturally provide an answer to the dark matter question. However, due the characteristically large relic abundance of the LSP's, the MSSM is also naturally susceptible to cosmological constraints, either because the relic density of LSP's is so large that it is in conflict with a gross cosmological feature, e.g. the age of the universe, or because one may be able to detect the interactions of the LSP with terrestrial detectors or detect the self-interactions of the LSP in the galactic halo or in the cores of the earth or the sun [3].

The MSSM contains in principle two neutral dark matter candidates, the sneutrino $\tilde{\nu}$, and the lightest neutralino $\tilde{\chi}^0$. The sneutrino, though, has

already been excluded[1] as a dark matter candidate by a combination of LEP bounds and direct detection experiments [4] . The lightest neutralino may be either gaugino-like (in particular $\widetilde{B}$-like) or Higgsino-like, and both the phenomenology and cosmology of neutralinos depend strongly on the neutralino composition. In this talk we will study the question of how viable these remaining MSSM dark matter candidates are in light of recent LEP data.

2. Neutralinos

In general, the neutralinos are linear combinations of the neutral gauginos and Higgsinos,

$$\chi_i = \beta_i \tilde{B} + \alpha_i \tilde{W} + \gamma_i \tilde{H}_1 + \delta_i \tilde{H}_2, \qquad i = 1, \ldots, 4 \tag{1}$$

In this notation, the gaugino purity of a neutralino χ_i is defined to be $\sqrt{\alpha_i{}^2 + \beta_i{}^2}$, and its Higgsino purity $\sqrt{\gamma_i{}^2 + \delta_i{}^2}$. In the $(\tilde{B}, \tilde{W}^3, \tilde{H}_1^0, \tilde{H}_2^0)$ basis, the neutralino mass matrix takes the form

$$\begin{pmatrix} M_1 & 0 & -M_Z s_\theta c_\beta & M_Z s_\theta s_\beta \\ 0 & M_2 & M_Z c_\theta c_\beta & -M_Z c_\theta s_\beta \\ -M_Z s_\theta c_\beta & M_Z c_\theta c_\beta & 0 & -\mu \\ M_Z s_\theta s_\beta & -M_Z c_\theta s_\beta & -\mu & 0 \end{pmatrix}, \tag{2}$$

where s_θ $(c_\theta) = \sin\theta_W$ $(\cos\theta_W)$, s_β $(c_\beta) = \sin\beta$ $(\cos\beta)$, and where gaugino mass unification implies $M_1 = 5/3 \tan^2\theta_W M_2$. The coefficients $\alpha_i, \ldots, \delta_i$ in (1) depend on $\tan\beta$ and on the soft SUSY-breaking mass parameters M_1, M_2 and μ, which appear in (2), and Fig. 1 displays the regions of high gaugino and Higgsino purity in the (μ, M_2) plane. In the limit $|\mu| \gg M_i$, the lightest neutralino is gaugino-like, specifically a $\tilde{B}$, i.e. $\beta_1 \approx 1$ in (1), and this is typically the case in mSUGRA and in models with gauge mediated supersymmetry breaking (GMSB). In Fig. 1, contours of constant $\tilde{B}$ purity are displayed as long-dashed lines. In the opposite limit, $M_i \gg |\mu|$, the lightest neutralino is Higgsino-like, and for small to moderate M_2, the lightest neutralino is the particular Higgsino combination defined by $\tilde{S}^0 \equiv \tilde{H}_1^0 \cos\beta + \tilde{H}_2^0 \sin\beta$, i.e., $\gamma = \cos\beta$ and $\delta = \sin\beta$, with $m_{\tilde{S}_0} \to \mu \sin 2\beta$ [7]. Contours of $\tilde{S}^0$ purity are displayed in Fig. 1 as dash-dotted lines. For large M_2, the lightest neutralino is the state $\tilde{H}_{12} \equiv \frac{1}{\sqrt{2}}(\tilde{H}_1^0 \pm \tilde{H}_2^0)$, i.e., $\delta = \pm\gamma = \pm 1/\sqrt{2}$ for $\text{sgn}(\mu) = \pm 1$, with $m_{\tilde{H}_{12}} \to |\mu|$ [8], and contours of $\tilde{H}_{12}$ purity are shown as short-dashed lines in Fig. 1.

---

[1] Outside the MSSM, these constraints may be evaded. See [5],[6].

In mSUGRA, the relationship between μ and M_2 is determined from the conditions of gaugino unification and sfermion and Higgs mass unification, along with the requirement of correct radiative electroweak symmetry breaking, and this relationship is shown in Fig. 1 as a thick solid line. As suggested above, the resulting contour lies in the gaugino region, and the heavier the neutralino, the more pure its $\widetilde{B}$ content. Also shown in Fig. 1 are contours of constant chargino mass, where 91 GeV represents the current LEP lower bound on $m_{\chi^\pm}$ [10], and constant neutralino mass. As a preview of the small size of the Higgsino dark matter region we'll be discussing, it consists of a subset of the shaded region between the $m_{\chi^\pm} = 91$ GeV and $m_\chi = M_W$ contours.
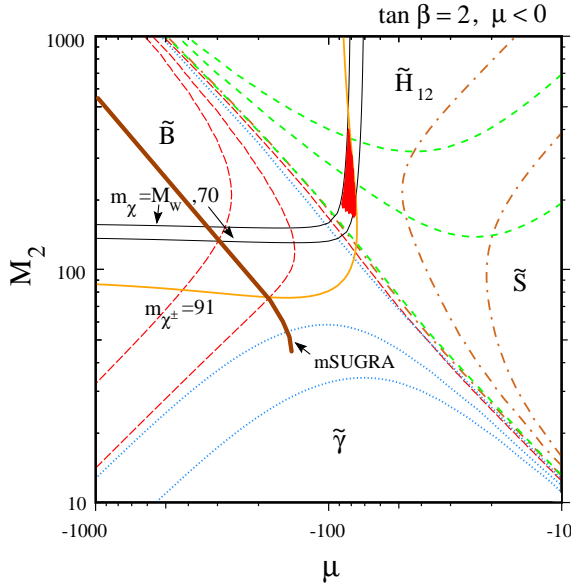

Figure 1. *Contours of neutralino purity: 99%, 97% and 75%, and chargino and neutralino masses (solid lines). The long-dashed lines are contours of high bino purity, the dotted lines are contours of high photino purity, the dashed lines are contours of high $\tilde{H}_{12}$ Higgsino purity, and the dash-dotted lines are contours of high $\tilde{S}_0$ Higgsino purity. Also shown are contours of constant m_χ and $m_{\chi^\pm}$ and the dependence of μ on M_2 in mSUGRA. We've taken $m_0 = 100$ GeV.*

3. LEP Bounds

Recent runs at LEP at center-of-mass energies of 172 and 183 GeV have excluded large areas of MSSM parameter space, and subsequent runs at

~ 190 and $200\,\text{GeV}$ will push the bounds even further. In this section we summarize the LEP bounds that we implement in this talk.

- Searches for chargino pair production at LEP 172 and LEP 183 have excluded chargino masses less than $86\,\text{GeV}$ [9] and $91\,\text{GeV}$[10] respectively, modulo two loopholes. The first loophole is relevant when the neutralino is a gaugino and occurs when the mass of the sneutrino is close to that of the chargino. The lower limit on $m_{\chi^\pm}$ is reduced as $m_{\tilde\nu}$ is reduced toward $m_{\chi^\pm}$ from above, due to destructive interference with the t-channel sneutrino exchange process, and then disappears entirely for $m_{\chi^\pm} > m_{\tilde\nu} \gtrsim m_{\chi^\pm} - 3\,\text{GeV}$, in which case $\tilde\chi^\pm$ decay is dominated by $\tilde\nu+$ soft lepton final states. Bounds on chargino production reappear when $m_{\chi^\pm} - m_{\tilde\nu} \gtrsim 3\,\text{GeV}$ and the lepton detection efficiency picks up again. The second loophole is relevant in the Higgsino region and occurs when $\Delta M = m_{\chi^\pm} - m_\chi$ is small, and it again is due to the reduction in detection efficiency when the mass difference between the produced particle and its supersymmetric decay product is small. The effect of each of these loopholes will be discussed in more detail later on.

- Searches for associated neutralino production can provide strong bounds when the neutralino is a Higgsino. In the Higgsino region of interest for this talk, associated neutralino production is dominated by $e^+e^- \to \chi\chi_{2,3,4}$ and corresponds essentially to $m_\chi + m_{\chi'_H} = 182\,\text{GeV}$, where χ'_H is the lightest mainly-Higgsino state among the $\chi_{2,3,4}$.

- Searches for Higgs production provide a lower limit of $m_h > 88\,\text{GeV}$ at low $\tan\beta$ [11]. Bounds from Higgs searches are particularly constraining at low $\tan\beta$, where the experimental bounds are strongest and where the tree level Higgs mass is small. Here radiative corrections to the Higgs mass [12] must be very large, leading to strong lower bounds on the masses of the sfermions, and in particular the stops. However, the extraction of the radiatively corrected Higgs mass in the MSSM has an uncertainty of $\sim 2\,\text{GeV}$, so we conservatively take $m_h > 86\,\text{GeV}$ as our experimental lower limit at low $\tan\beta$.

- We also implement bounds coming from searches for sfermion production, in particular slepton [13] and stop production [14], as well as constraints on the sneutrino mass from the Z width [17].

4. Gaugino Dark Matter

As we have seen above, the lightest neutralino tends in many instances to be a $\widetilde{B}$, as is the case in mSUGRA, in particular. For our numerical examples,

4

we will restrict our attention to mSUGRA, although the qualitative features apply to more general cases, so long as the LSP is a $\widetilde{B}$. The relic abundance of neutralinos is given by

$$\Omega_\chi h^2 \sim \frac{3 \times 10^{-10}\,\mathrm{GeV}^{-2}}{\langle \sigma_{\mathrm{ann}} v \rangle} < 0.3, \tag{3}$$

where $\langle \sigma_{\mathrm{ann}} v \rangle$ is the thermally averaged neutralino annihilation cross-section at the time the neutralinos fall out of chemical equilibrium with the thermal bath. The inequality in (3) comes from the requirements that the age of the universe t_U be greater than 12 Gyr and that the total $\Omega < 1$.

In the early universe, $\widetilde{B}$ annihilation is typically dominated by sfermion exchange into fermion pairs (Fig. (2)). Due to the Majorana nature of the neutralinos, this process generally exhibits a p-wave suppression [1] (but see [15, 16]) which decreases $\langle \sigma_{\mathrm{ann}} v \rangle$, and increases $\Omega_\chi h^2$, by roughly an order of magnitude. Now, as the sfermion masses are increased, the relic abundance of neutralinos increases, and for sufficiently heavy sfermions, $\Omega_\chi h^2$ violates the bound (3). Thus the requirement that $t_U > 12$ Gyr translates into an upper bound on the sfermion masses.
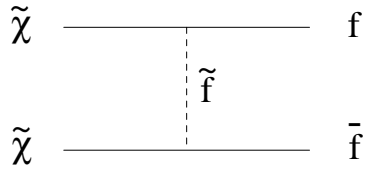

Figure 2. *The dominant contribution to $\widetilde{B}$ annihilation.*

In mSUGRA, the sfermion and gaugino masses are given by

$$m_{\tilde{f}}^2 \;=\; m_0^2 + C_{\tilde{f}}\, m_{1/2}^2 + O(m_Z^2), \tag{4}$$
$$(M_1, M_2) \;\approx\; (0.4, 0.8)\, m_{1/2}, \tag{5}$$

where m_0 and $m_{1/2}$ are the common scalar and gaugino mass parameters, and the coefficients $C_{\tilde{f}}$ are determined by the RGE evolution of the sfermion masses from the unification scale to the electroweak scale. The remaining parameters in mSUGRA are the common trilinear scalar mass parameter A_0, which appears in the sfermion mass matrices, $\tan\beta$, and the sign of μ. The magnitude of μ is fixed in mSUGRA by the conditions of correct electroweak symmetry breaking, as seen in Fig. 1. The sfermion masses are typically insensitive to A_0, so in mSUGRA, the bound on t_U translates simply into a upper bound on m_0 and $m_{1/2}$. Because the cosmological constraint provides upper limits on the soft masses, whereas particle

5

searches typically give lower limits on the same parameters, the two types of constraints are nicely complementary. Lastly, the Higgs mass is given by

$$m_h^2 = m_Z^2 \cos^2 2\beta \ + \ \text{rad. corr.} \, (m_{\tilde{t}_i}^2, m_t, A_t), \qquad (6)$$

where the dominant part of the radiative corrections depends logarithmically on the stop masses. At low $\tan\beta$, the tree level Higgs mass is small, and the Higgs mass constraint then imposes severe lower bounds on the stop masses, which translates into lower bounds on $m_{1/2}$ and m_0.

Fig. 3 summarizes [18] the LEP 172 constraints on the mSUGRA parameter space for $\tan\beta = 2$, $\mu < 0$. The solid contour at the left of the figure represents the combined chargino and slepton bounds[2]. At large m_0, the chargino bound reaches the kinematic limit, but as m_0 is decreased, the sneutrino mass falls, and the first loophole described in section 3 reduces the bound below 86 GeV. At $m_0 \sim 75$ GeV, the sneutrino mass drops below that of the chargino, and the bound retreats rapidly to the left; at lower m_0, the slepton bound comes into play and shuts the door to lower $m_{1/2}$. At this relatively low value of $\tan\beta$, both the chargino and slepton bounds are dominated by the Higgs mass constraint (~ 76 GeV), shown as the thick solid line stretching almost vertically at $m_{1/2} \sim 250$ GeV. For lower values of $\tan\beta$, the Higgs bound moves rapidly to the right, whereas for higher $\tan\beta$, the chargino bound moves to the right, and the Higgs bound retreats to the left and crosses beneath the combined chargino/slepton bound at $\tan\beta \sim 3$.

It is interesting to consider how low a neutralino mass these combined constraints admit. The Higgs bound forces one to very large $m_{1/2}$ at low m_0, giving a heavy neutralino; however, one can make the stops heavy by taking m_0 very large, rather than $m_{1/2}$, and so the Higgs contour does bend to the left at very large m_0 and strikes the chargino contour. At $\tan\beta = 2$, this occurs at $m_0 \sim 800$ GeV. Consequently, in the absence of an independent upper limit on m_0, the lower bound on m_χ is set by the intersection of the Higgs contour with the chargino contour at large m_0 and yields a minimum neutralino mass of 42 GeV. Fig. 4 displays [18] the lower bound on m_χ as a function of $\tan\beta$, given different sets of theoretical and experimental constraints. The purely experimental lower bound (i.e. not yet using cosmology) in mSUGRA is given by the solid line labelled UHM (as a reminder that it is the Unification of the Higgs Masses with the sfermion masses which leads to $|\mu|$ being an output, rather than an input, in mSUGRA).

The dark shaded area in Fig. 3 delimits the cosmologically preferred region with $0.1 < \Omega_\chi h^2 < 0.3$. The upper limit, as described above, comes

---

[2] All the curves in Fig. 3 are computed using tree level neutralino and chargino masses. They shift by a few GeV when 1-loop radiative corrections to the masses are included.
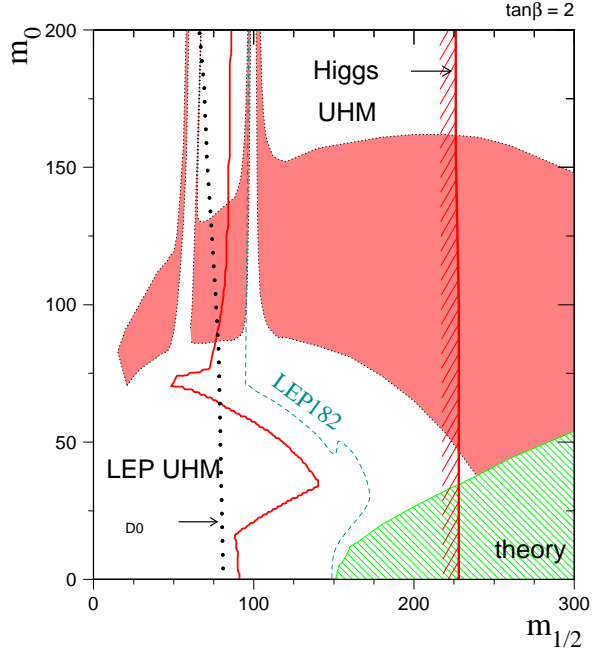
Figure 3. *We display for $\mu < 0$ and $\tan\beta = 2$ the domains of the $(m_{1/2}, m_0)$ plane that are excluded by the LEP 172 chargino and selectron searches in mSUGRA, the domains that are excluded by Higgs searches, the regions that are excluded cosmologically because $m_{\tilde\tau_R} < m_\chi$, and the domains that have relic neutralino densities in the favoured range $0.1 < \Omega_\chi h^2 < 0.3$*

from an upper bound on the age of the universe. The lower limit is less a bound *per se* than a preference, stemming from the desire to have the neutralinos comprise a significant fraction of the dark matter. The two narrow vertical channels at $m_{1/2} \sim 65\,\mathrm{GeV}$ and $m_{1/2} \sim 100\,\mathrm{GeV}$ arise from s-channel neutralino annihilation on the Higgs and Z^0 poles, respectively. Note that top of the shaded area continues to fall for $m_{1/2} > 300\,\mathrm{GeV}$, and it intersects with the "theory" excluded area (where a stau is the LSP) at $m_{1/2} \sim 425\,\mathrm{GeV}$. Thus, as advertised, $\Omega_\chi h^2 < 0.3$ yields an upper bound on both m_0 and $m_{1/2}$. This independent upper bound on m_0 forbids the large m_0 solution to the Higgs mass constraint (modulo a very narrow region on the Z^0 pole) and dramatically increases the lower bound on the neutralino mass for values of $\tan\beta$ where the Higgs mass bound is significant. This is seen in Fig. 4, where the branch of the solid curve labelled "cosmo+UHM" is the result of including both the constraints from particle searches at LEP 172 and the requirement $\Omega_\chi h^2 < 0.3$.
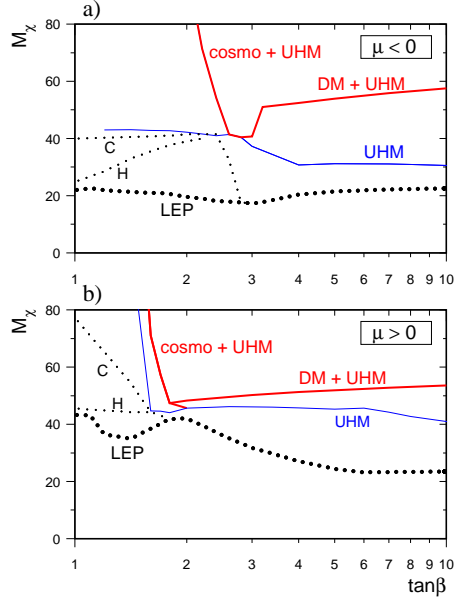
7

Figure 4. *Various lower limits on m_χ using different experimental and theoretical inputs are compared, as functions of $\tan\beta$, for both (a) $|\mu| < 0$ and (b) $|\mu| > 0$. The solid curves represent bounds in mSUGRA, including purely experimental bounds ("UHM"), separately augmented by cosmological ("cosmo+UHM") and dark matter ("DM+UHM") constraints. The dotted curves show the impact of Higgs (H) and cosmological (C) constraints in the MSSM.*

Further, for low enough $\tan\beta$, the Higgs bound moves entirely to the right of the dark-shaded region, and for $\mu < 0$, the cosmologically allowed range[3] with $\Omega_\chi h^2 < 0.3$ is actually *incompatible* with the Higgs lower limit on $m_{1/2}$ for $\tan\beta \lesssim 1.7$. We conclude that in mSUGRA there is no range of $m_{1/2}$ compatible with all the constraints provided by the LEP 172 particle searches and the upper bound on the cosmological relic density, for sufficiently small $\tan\beta \lesssim 1.7$. Hence, *there is a lower bound* $\tan\beta \gtrsim 1.7$, if all these constraints are applied simultaneously. Similarly, for $\mu > 0$, the bound from the LEP 172 searches is $\tan\beta \gtrsim 1.4$. These bounds have since improved. Updated chargino and slepton contours from LEP 183 are shown as dashed lines in Fig. 3. The chargino contour displayed is the kinematic limit of 91 GeV, and as discussed above, overestimates the chargino bound for low m_0. The LEP 183 Higgs bound is off the right side of the figure and in fact is very close to the intersection point of the $\Omega_\chi h^2 < 0.3$

---

[3] The cosmological upper bound on $m_{1/2}$ varies only weakly with $\tan\beta$ for $\tan\beta \lesssim 2$.

8

and "theory" contours. The LEP 183 Higgs bound then combines with the cosmological constraint to yield the updated [19] lower bounds

$$\tan\beta \gtrsim \left\{ \begin{array}{ll} 2.0 & \mu < 0 \\ 1.65 & \mu > 0 \end{array} \right. \tag{7}$$

Lastly, the branch of the solid curve labelled "DM+UHM" in Fig. 4 exhibits the effect of additionally including the constraint that there be a significant amount of neutralino dark matter, $\Omega_\chi h^2 > 0.1$. As $\tan\beta$ is increased, the chargino bound moves to the right, as does the Higgs pole, and the Higgs and Z_0 poles widen, eventually merging to form one large pole region, at $\tan\beta \sim 3$. The kink in the "DM+UHM" line emerges from the necessity to sit on the right side of the combined pole region, after the merging, in order to have sufficient dark matter.

5. Higgsino Dark Matter

5.1. Introduction

As shown in Fig. 1, when the neutralino is a Higgsino, it approaches the particular combination $\tilde{H}_{12}$. There are in principle two regions in the (μ, M_2) plane where $\tilde{H}_{12}$ can provide an interesting relic density. For large M_2, they correspond to $|\mu| < M_W$ but with $m_{\chi^\pm}$ above the LEP limit, and $|\mu| \gtrsim 1$ TeV [8, 20]. The intermediate-mass Higgsino states are not of cosmological interest, because of their rapid annihilations to W and Z pairs. We have little to add concerning the very heavy $\tilde{H}_{12}$ states, but the lighter Higgsinos lie directly in the region where the current LEP runs are eating away at the parameter plane, and thus it is of interest to examine how much of the light Higgsino parameter space remains consistent with the LEP bounds.

In the far Higgsino limit, the chargino and neutralino spectrum simplifies, and for $M_2 \gg |\mu|$,

$$\begin{array}{ccc} m_{\chi_1^0} & \approx \; m_{\chi_2^0} \; \approx & |\mu| \\ m_{\chi^\pm} & \approx & |\mu|, \end{array} \tag{8}$$

A non-zero gaugino component provides some splitting of the spectrum, and at tree level,

$$m_{\chi_1^0} \; < \; m_{\chi^\pm} \; < \; m_{\chi_1^0}. \tag{9}$$

The LEP 182 lower bound of 91 GeV on the chargino mass then imposes a comparable lower bound on m_χ in the limit of pure Higgsinos. However, if $m_\chi > m_W$, the annihilation channel $\tilde{\chi}^0 \tilde{\chi}^0 \to W^+ W^-$ is available to

neutralinos at their time of decoupling in the early universe. Neutralinos in fact love to annihilate into W pairs, since this process is not p-wave suppressed, in contrast to neutralino annihilation into fermion pairs, and so $\Omega_\chi h^2 \sim \langle \sigma_{\mathrm{ann}} v \rangle^{-1}$ is greatly reduced above the W threshold. Consequently, Higgsinos with masses above m_W (and below $\sim 1\,\mathrm{TeV}$) are not viable dark matter candidates. For this reason, LEP chargino searches are fatally squeezing Higgsino dark matter. In this section we examine over how much of the MSSM parameter space Higgsino dark matter remains viable, and comment on the fate of Higgsino dark matter when the last LEP runs are complete.

5.2. Loop Corrections to Ino Masses

Constraints on Higgsino dark matter are sensitive to loop corrections to the neutralino and chargino masses, and this sensitivity appears in two separate pieces of the analysis. First, as mentioned in section 3, there is a loophole which appears in the chargino experimental bounds when the mass of the chargino is close to the mass of the neutralino, and looking at eqn. 8, this is exactly the case in the Higgsino limit, where the chargino and neutralino masses are both close to $|\mu|$. The second panel of Fig. 5 displays [19] the LEP 172 lower bound on the chargino mass as a function of $\Delta M = m_{\chi^\pm} - m_\chi$, for $\tan\beta = 2$ and $m_0 = 200\,\mathrm{GeV}$. Characteristically, the bound on $m_{\chi^\pm}$ drops for small ΔM, and essentially disappears for $\Delta M < 5\,\mathrm{GeV}$. The first panel in Fig. 5 displays the chargino bound as a function of M_2, where $|\mu|$ is fixed by the chargino mass. For larger M_2 the neutralino is more pure Higgsino, the masses of the chargino and neutralino are more degenerate, and the bound on $m_{\chi^\pm}$ drops.

Since the chargino bounds are closely dependent on ΔM, it is important to consider the 1-loop radiative corrections to the neutralino and chargino masses in the Higgsino region. The 1-loop corrections to the neutralino and chargino masses have been computed [21, 22, 23], and a comparison of the dotted and solid curves in Fig. 5 shows their effect on the chargino bound. As expected, at large M_2, where ΔM is small, the effect is significant, while for $M_2 \leq 400\,\mathrm{GeV}$, there is little effect. The overlap of the two curves in the second panel of Fig. 5 demonstrates that it is really the quantity ΔM to which the chargino bound is sensitive.

The second piece of the analysis which is sensitive to the radiative corrections is the computation of the Higgsino relic abundance. Unlike in the gaugino case, the approximate degeneracy of the neutralino and chargino spectrum (8) in the Higgsino region requires the inclusion of the next-to-lightest and next-to-next-to-lightest states and their co-annihilations with the LSP (and self-annihilations) in the calculation of $\Omega_\chi h^2$ [24, 25]. That this effect is particularly important is due again to the p-wave suppression
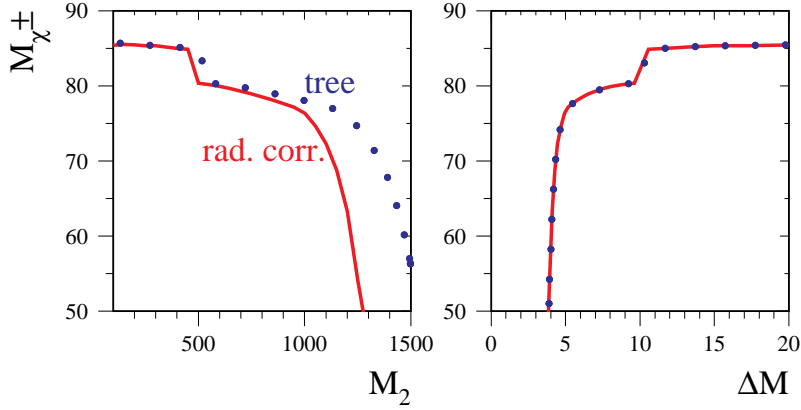
10

Figure 5. *The experimental limit on $m_{\chi^\pm}$ as function of M_2 and as a function of $\Delta M \equiv m_{\chi^\pm} - m_\chi$, for fixed $m_0 = 200\,\mathrm{GeV}$ and $\tan\beta = 2$. The dotted line comes from a tree-level analysis, and the solid line is obtained using an ad hoc parameterization of the experimental efficiency, in conjunction with the radiatively-corrected mass formulae.*

of the annihilation of neutralinos into fermions. Expanding the thermally averaged annihilation cross-section in powers of (T/m_χ),

$$\langle \sigma_{\mathrm{ann}} v \rangle_T = A + B\,(T/m_\chi) + \ldots, \tag{10}$$

one finds the zeroth order piece A suppressed by m_f^2. Neutralinos with masses of interest for dark matter fall out of chemical equilibrium with the thermal bath when the temperature is $\sim (1/20 - 1/25) \times m_\chi$, so the effect of p-wave suppression, then, is an order of magnitude reduction in the annihilation rate. By contrast, the co-annihilation processes

$$\tilde\chi_1^0\,\tilde\chi_1^\pm \;\longrightarrow\; e^+\nu,\; \ldots$$
$$\tilde\chi_1^0\,\tilde\chi_2^0 \;\longrightarrow\; f\bar f$$

do not involve the annihilation of identical particles and so do not exhibit p-wave suppression. However, the number density of the heavier scattering states is Boltzmann suppressed at low temperatures, and so the ratio of co-annihilation to annihilation rates goes as

$$R_{\tilde\chi_1^0\tilde\chi_1^\pm}/R_{\tilde\chi_1^0\,\tilde\chi_1^0} \;\sim\; (T/m_\chi)\,e^{-\Delta M/T} \;\sim\; 25\,e^{-25(\Delta M/m_\chi)}, \tag{11}$$

and similarly for $\tilde\chi_1^0\,\tilde\chi_2^0$ co-annihilation[4]. For a degenerate spectrum, this amounts to better than an order of magnitude increase in the annihilation

---

[4] There are additional factors which suppress the annihilation rate for Higgsinos and increase the ratio $R_{\tilde\chi_1^0\tilde\chi_1^\pm}/R_{\tilde\chi_1^0\,\tilde\chi_1^0}$.

rate, whereas if the mass difference $\Delta M/m_\chi$ is as much as 25 percent, this ratio of rates is less than 0.05. Clearly there is a tremendous sensitivity of $\Omega_\chi h^2$ to ΔM, and consequently to the radiative corrections to the chargino and neutralino masses.

Lastly, we note that the loophole in the chargino bound occurs for small ΔM, where co-annihilations typically make the Higgsino relic abundance tiny. By contrast, the relic density turns out to be significant only for larger ΔM, where the chargino bounds are strongest. It is therefore difficult to wriggle out of the the chargino mass constraints by appealing to this loophole in the chargino limits, while still preserving Higgsino dark matter.

5.3. The Fate of Higgsino Dark Matter

We now explore the Higgsino dark matter regions which survive the LEP bounds. In order to conservatively estimate their area in the following, we take a large sfermion mass $m_0 = 1\,\mathrm{TeV}$. This has both the effect of minimizing the impact of the Higgs mass constraint by producing large radiative corrections to the Higgs mass and of minimizing the contributions to neutralino annihilation through the neutralino's (small) gaugino component. We take a large pseudoscalar mass $m_A = 1\,\mathrm{TeV}$, similarly to give a large Higgs tree-level mass and to minimize the effect of s-channel pseudoscalar annihilation. We take A_t at the quasi-fixed point $\sim 2.25\,M_2$. This is a very good approximation at low $\tan\beta$, and the small flexibility one has to vary A_t at larger $\tan\beta$ doesn't substantially impact the allowed dark matter regions. Lastly, our working definition of a Higgsino is that $p^2 = \gamma_i^2 + \delta_i^2 > 0.81$. We note that since Higgsino and gaugino purities add in quadrature to 1, a Higgsino purity of 0.9 (our choice) corresponds to a gaugino purity of 0.44, so our choice is not too restrictive.

In Fig. 6a we display [19] for $\mu < 0$ contours of constant chargino mass $m_{\chi^\pm} = 91\,\mathrm{GeV}$, $m_\chi + m_{\chi'_H} = 182\,\mathrm{GeV}$, Higgs mass m_h, and Higgsino purity, along with a contour of constant $\Omega_\chi h^2 = 0.1$, for $\tan\beta = 2$. We see that the dashed lines in Fig. 6a representing the chargino and associated neutralino mass contours bound one away from small $|\mu|$, while the Higgs mass limit bounds one away from small M_2. The latter is particularly restrictive at low $\tan\beta$, where the tree-level Higgs mass is small, and thus where radiative corrections to m_h must be enhanced by taking large stop masses. The solid contour contains the region which leads to a significant neutralino relic density $\Omega_\chi h^2 \geq 0.1$, and its limited range in M_2 is a result of co-annihilations. For larger values of M_2, the neutralino is a purer Higgsino, and the masses of both the lightest chargino and the next-to-lightest neutralino approach the neutralino mass from above, enhancing the effect of co-annihilations that deplete the relic Higgsino abundance. For larger values of $|\mu|$, the relic density is suppressed by annihilations into W pairs. The hashed contours in Fig. 6a represent Higgsino purities. Note
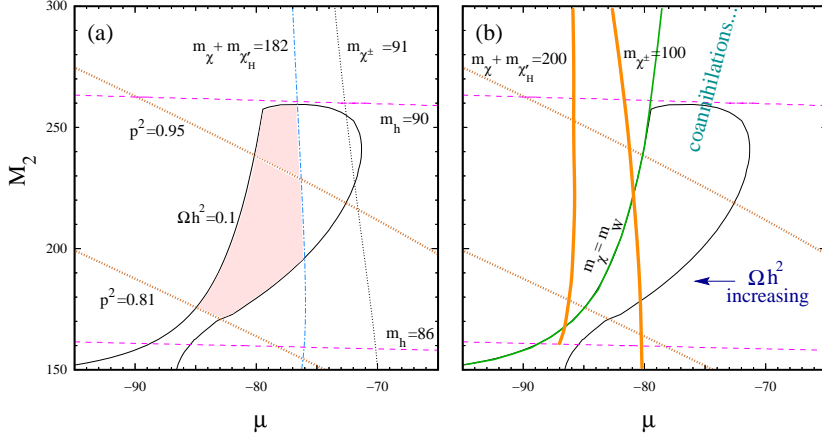
12

Figure 6. *Survey of experimental and cosmological constraints in the μ, M_2 plane, focusing on Higgsino dark matter for tanβ = 2 and μ < 0 In a) we plot the radiatively-corrected contours for $m_{\chi^\pm} = 91$ GeV, for $m_\chi + m_{\chi'_H} = 182$ GeV, for selected values of m_h and the Higgsino purity p, and for $\Omega_\chi h^2 = 0.1$. The shaded regions yield a Higgsino which satisfies the mass and relic density constraints described in the text. In b) we show the expected bounds from LEP 200.*

the limited range of μ for which the mass and relic density constraints are satisfied.

The combined effects of the above constraints, corresponding to the shaded regions of Fig. 6, are displayed for different values of $\tan\beta$ in Fig. 7. We find that there are no consistent Higgsino dark matter candidates for $\tan\beta \leq 1.8$ or ≥ 2.5 for $\mu < 0$, or for any value of $\tan\beta$ for $\mu > 0$. The Higgs mass constraint cuts off the bottom of the allowed regions at low $\tan\beta$. When $\mu < 0$ it becomes a relevant constraint for $\tan\beta < 2.0$ (its effect can be seen in the flat lower edge of the $\tan\beta = 1.9$ contour) and is responsible for the complete disappearance of the allowed region when $\tan\beta \leq 1.8$. Within the allowed regions displayed, the relic densities generally increase as $|\mu|$ is increased, until the neutralino mass, whose minimum value here is ~ 71 GeV, becomes greater than m_W, at which point the W^+W^- annihilation channel opens, driving the relic $\Omega_\chi h^2$ below 0.1. In Fig. 6b, we plot the contour $m_\chi = m_W$, which makes evident the drop in $\Omega_\chi h^2$ above the W pair threshold[5] . In any event, $\Omega_\chi h^2$ is never greater than 0.12 anywhere in the allowed regions for $\mu < 0$.

In Fig. 6b we show the same plot as Fig. 6a, but with an estimate of the bounds that should be achieved at LEP's eventual run at ~ 200 GeV

---

[5] Sub-threshold annihilation of neutralinos, not included in this analysis, exclude a further slice of Higgsino dark matter on the right-hand side of the $m_\chi = m_W$ contour[26].
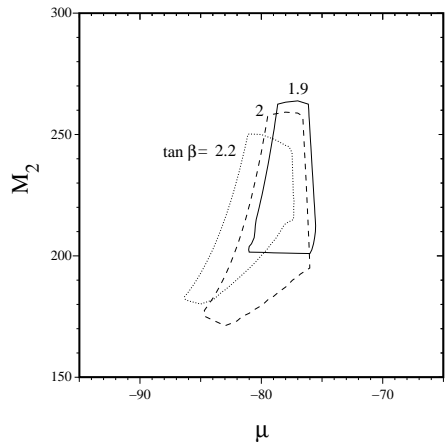
Figure 7. *The regions of the μ, M_2 plane allowed by the constraints shown in the previous figure are shown for several different values of tanβ. There are no consistent choices of Higgsino parameters for $\tan\beta < 1.8$ or > 2.5 for $\mu < 0$, or for any value of $\tan\beta$ for $\mu > 0$.*

center-of-mass energy. We see that the associated neutralino production bound of $m_\chi + m_{\chi'_H} = 200\,\text{GeV}$ excludes entirely the remaining allowed Higgsino dark matter region at $\tan\beta = 2$ for $\mu < 0$. It is also apparent that at this value of $\tan\beta$, the projected Higgs mass bound of $\sim 105\,\text{GeV}$, which lies well off the top of the plot, will play the same role. And, in fact, the entire set of allowed Higgsino dark matter regions displayed in Fig. 7 for all $\tan\beta$ are excluded by either one of the conditions $m_h > 100\,\text{GeV}$ or $m_\chi + m_{\chi'_H} > 200\,\text{GeV}$ alone. The first of these bounds should be achieved even if LEP falls somewhat shy of 200 GeV in its final run.

In Fig. 8 we show the equivalent plot to Fig. 6a, for $\mu > 0$; in this case the Higgsino purities are lower, and the entire dark matter region falls below the purity cutoff. This turns out to be the case for all $\tan\beta$; that is, for all values of $\tan\beta$, the only regions of parameter space for $\mu > 0$ which have a significant amount of neutralino dark matter $\Omega_\chi h^2 > 0.1$ have either a mixed or gaugino-like lightest neutralino. Lastly, we find the Higgsino dark matter regions are even more restricted for both $\mu < 0$ and $\mu > 0$ if the gaugino masses are related by $M_1 = M_2$ [27]. For a more detailed discussion of both the $\mu < 0$ and $\mu > 0$ cases, see reference [19].

6. Summary and Outlook

We've seen that R-parity conserving SUSY models still provide a good dark matter candidate. Neutralinos are of particular cosmological interest
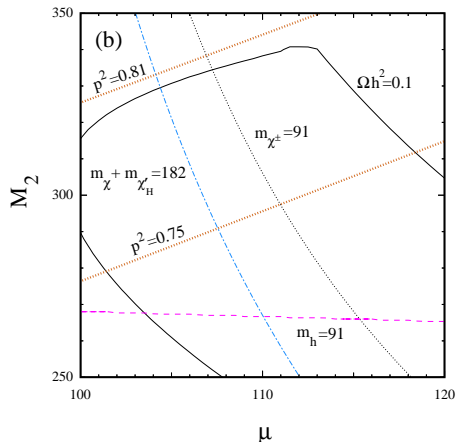
14

Figure 8. *Same as Fig. 6a for $\mu > 0$*

when the lightest neutralino is a gaugino, in particular a bino, and current experiments are probing into the heart of the gaugino dark matter region. Cosmological constraints combine neatly with experimental bounds, and taken together they exclude all values of $\tan\beta < 2$ (1.65) for $\mu < 0$ (> 0) in mSUGRA. By contrast, Higgsino dark matter is being fatally squeezed by LEP. Already small, restricted to an area $\sim 10\,\text{GeV}$ wide in μ and for only $\tan\beta$ between 1.8 and 2.5 for $\mu < 0$, the remaining Higgsino dark matter regions (with masses $< 1\,\text{TeV}$) will be finally excluded by either of the conditions $m_h > 100\,\text{GeV}$ or $m_\chi + m_{\chi'_H} > 200\,\text{GeV}$, bounds which should be achieved by LEP 200.

References

[1] H. Goldberg, *Phys. Rev. Lett.* **50** (1983) 1419;

[2] J. Ellis, J.S. Hagelin, D.V. Nanopoulos, K.A. Olive and M. Srednicki, *Nucl. Phys.* **B238** (1984) 453.

[3] For a review of detection schemes, see G. Jungman, M. Kamionkowski, and K. Greist, *Phys. Rep.* **267** (1996) 195.

[4] T. Falk, K. A. Olive, M. Srednicki, *Phys. Lett.* **339** (1994) 248.

[5] L. J. Hall, T. Moroi, H. Murayama,*Phys. Lett.* **424** (1998) 305.

[6] T. Han, R. Hempfling, *Phys. Lett.* **415** (1997) 161.

[7] J. Ellis, J.S. Hagelin, D.V. Nanopoulos, K.A. Olive and M. Srednicki, *Nucl. Phys.* **B238** (1984) 453.

[8] K.A. Olive and M. Srednicki, *Phys. Lett.* **B230** (1989) 78; *Nucl. Phys.* **B355** (1991) 208; K. Greist, M. Kamionkowski and M.S. Turner, *Phys. Rev.* **D41** (1990) 3565.

[9] ALEPH Collaboration, D.Buskulic et al., *Phys. Lett.* **B373** (1996) 246; OPAL Collaboration, G. Alexander et al., *Phys. Lett.* **B377** (1996) 181.; L3 Collaboration, M. Acciarri et al., *Phys. Lett.* **B377** (1996) 289;; DELPHI Collaboration, P. Abreu et al., *Phys. Lett.* **B382** (1996) 323 .

[10] Presentations at the open LEPC session, Nov. 11th, 1997: ALEPH collaboration, P. Dornan, `http://alephwww.cern.ch/ALPUB/seminar/seminar.html`; DELPHI collaboration, P. Charpentier, `http://wwwinfo.cern.ch/∼charpent/LEPC/`; L3 collaboration, M. Pohl, `http://hpl3sn02.cern.ch/conferences/talks97.html`; OPAL collaboration, A. Honma, `http://www.cern.ch/Opal/`.

[11] see. e.g. L3 Collaboration, CERN Preprint CERN-EP98-72 (1998).

[12] H.E. Haber, R. Hempfling and A.H. Hoang, *Z. Phys.* **C75** 539; see also M. Carena, M. Quiros and C.E.M. Wagner, *Nucl. Phys.* **B461** (1996) 407.

[13] ALEPH Collaboration, R. Barate et al., CERN preprint EP/98-077 (1998).

[14] OPAL collaboration, K. Ackerstaff et al., CERN preprint PPE/97-046 (1997).

[15] T. Falk, R. Madden, K. A. Olive, M. Srednicki, *Phys. Lett.* **B318** (1993) 354.

[16] T. Falk, K. A. Olive, M. Srednicki , *Phys. Lett.* **B354** (1995) 99.

[17] J. Ellis, T. Falk, K.A. Olive and M. Schmitt, *Phys. Lett.* **B388** (1996) 97.

[18] J. Ellis, T. Falk, K.A. Olive and M. Schmitt, *Phys. Lett.* **B413** (1997) 355.

[19] J. Ellis, T. Falk, G. Ganis, K.A. Olive and M. Schmitt, hep-ph/9801445.

[20] P. Gondolo, J. Edsjo, hep-ph/9804459.

[21] A.B. Lahanas, K. Tamvakis and N.D. Tracas, *Phys. Lett.* **B324** (1994) 387.

[22] D. Pierce and A. Papadopoulos, *Phys. Rev.* **D50** (1994) 565 and *Nucl. Phys.* **B430** (1994) 278.

16

[23] D.M. Pierce, J.A. Bagger, K. Matchev and R.-J. Zhang, *Nucl. Phys.* **B491** (1997) 3.

[24] K. Griest and D. Seckel, *Phys. Rev.* **D43** (1991) 3191.

[25] S. Mizuta and M. Yamaguchi, *Phys. Lett.* **B298** (1993) 120.

[26] M. Drees, M.M. Nojiri, D.P. Roy and Y. Yamada, Phys. Rev. **D56** (1997) 276.

[27] G.L. Kane and James D. Wells, Phys. Rev. Lett. **76** (1996) 4458.